

See discussions, stats, and author profiles for this publication at: <https://www.researchgate.net/publication/332969444>

Enhanced phased array imaging through reverberating interfaces

Conference Paper in AIP Conference Proceedings · May 2019

DOI: 10.1063/1.5099833

CITATIONS

0

READS

37

6 authors, including:



Marcus Ingram

KU Leuven

6 PUBLICATIONS 1 CITATION

[SEE PROFILE](#)



Anthony Mulholland

University of Strathclyde

101 PUBLICATIONS 448 CITATIONS

[SEE PROFILE](#)



Jerzy Dziewierz

University of Strathclyde

26 PUBLICATIONS 85 CITATIONS

[SEE PROFILE](#)

Some of the authors of this publication are also working on these related projects:



UK Research Centre in NDE (RCNDE) - Future Transducer Technologies [View project](#)



Generation, Detection & Analysis of Optimally Coded Ultrasonic Waveforms [View project](#)

Enhanced phased array imaging through reverberating interfaces

Cite as: AIP Conference Proceedings **2102**, 100005 (2019); <https://doi.org/10.1063/1.5099833>
Published Online: 08 May 2019

Marcus Ingram, Anthony Gachagan, Anthony J. Mulholland, Alison Nordon, Jerzy Dziewierz, and Martin Hegarty



View Online



Export Citation

ARTICLES YOU MAY BE INTERESTED IN

[Effect of surface compensation for imaging through doubly-curved surfaces using a 2D phased array](#)

AIP Conference Proceedings **2102**, 100008 (2019); <https://doi.org/10.1063/1.5099836>

[Uncertainty sensitivity analysis of damage tolerance evaluation with ultrasonic data](#)
AIP Conference Proceedings **2102**, 100004 (2019); <https://doi.org/10.1063/1.5099832>

[Machine learning and NDE: Past, present, and future](#)

AIP Conference Proceedings **2102**, 090001 (2019); <https://doi.org/10.1063/1.5099819>

AIP | Conference Proceedings

Get **30% off** all
print proceedings!

Enter Promotion Code **PDF30** at checkout



Enhanced Phased Array Imaging Through Reverberating Interfaces

Marcus Ingram^{1,a)}, Anthony Gachagan¹, Anthony J Mulholland², Alison Nordon³, Jerzy Dziewierz¹ and Martin Hegarty⁴

¹*Department of Electronic and Electrical Engineering, University of Strathclyde, Glasgow, UK.*

²*Department of Mathematics and Statistics, University of Strathclyde, Glasgow, UK.*

³*Department of Pure and Applied Chemistry, University of Strathclyde, Glasgow, UK.*

⁴*BP Chemicals Limited, Hull, UK.*

^{a)}Corresponding author: m.ingram@strath.ac.uk

Abstract. A key challenge to achieve non-invasive industrial process analysis is the transmission of information through the vessel wall. Typical non-invasive technologies, such as Raman spectroscopy, require an optically transparent ‘window’ into the process to acquire the process data. In this work, ultrasonic phased arrays were used to image a dynamic process through planar steel vessel walls into a fluid load. Due to the acoustic impedance mismatch at the steel-fluid interface, only a small fraction of the excitation energy comes back to the receiver in the form of useful echoes from the process. Also, the ultrasonic energy that is not transmitted across the steel-fluid interface reverberates within the vessel wall, masking signals that are reflected from within the process. Here, the ultrasonic array was deployed using Full Matrix Capture (FMC) followed by the Total Focusing Method (TFM) that focusses the ultrasonic beam at every pixel in the image. However, the TFM algorithm is not spatial resolved, leading to multiples of the reverberations interfering throughout the desired image region. To extract the signals corresponding to the process fluid, a method has been developed called the Reverberation Pattern Gain Correction Method (RP-GCM). Firstly, the algorithm uses ray-tracing to predict the path length of reverberations from the steel-fluid interface. The signals in the FMC data set corresponding to those reverberations are then windowed and a gain filter applied, prior to application of the regular TFM process. The RP-GCM has been applied to a simulated FMC data set, developed in PZFlex (OnScale, USA). Initial results demonstrate the effectiveness of this method in separating the vessel reverberations from the ultrasonic echoes of interest relating to the process.

INTRODUCTION

Ultrasonic phased arrays are typically deployed to non-invasively image into solid structures, for example for defect detection in non-destructive evaluation [1, 2] or medical diagnosis of patients [3]. Ultrasound imaging has a specific advantage over optical-based methods as it can image into optically opaque materials [1]. Recent technological advances in multiple-channel Phased Array Controllers (PAC) and General Purpose Graphics Processing Units (GP-GPU) have accelerated data acquisition and image construction algorithms, which has created the opportunity to apply ultrasonic imaging to dynamic systems such as industrial process analysis.

A key challenge to achieve non-invasive industrial process analysis is the transmission of information through the solid and typically opaque vessel wall. In this paper, a methodology is proposed to generate images of an industrial process stream through a steel vessel wall using standard ultrasonic data acquisition and imaging tools. At the interface between the steel and the process fluid, there is a large acoustic impedance mismatch that results in a strongly reflecting acoustic boundary at this interface. Approximately 87.5 % of the ultrasonic energy injected into the system is reflected at this acoustic boundary. Therefore, any signals reflected from within the process fluid are inherently weak relative to the amplitude of signals reflected from the acoustic boundary. In addition, the ultrasonic energy reflected at this acoustic boundary reverberates within the steel vessel wall, masking signals reflected from the process fluid.

Non-invasive through-steel ultrasonic measurement has been previously applied to industrial process analysis through quantification of the reverberation attenuation in the steel [4]. The reverberations were used to estimate the transmission coefficient at the steel-fluid interface, which led to the determination of the fluid density inside the pipe.

However, this was not a direct measurement of the process and was only achieved using single element transducers, so imaging of the process was not possible.

Other examples of non-invasive ultrasonic measurement in industrial process analysis have typically used Perspex [5, 6] that has an acoustic impedance much closer to water. The benefit of this is twofold; the Perspex promotes the transmission of ultrasonic energy across the vessel-fluid interface and in addition it reduces the amplitude of reverberations within the vessel wall relative to reflections from the process fluid. However, this requires modification of the vessel structure that is not always practical in an industrial plant.

An alternative solution has been proposed in the medical field to transmit ultrasound non-invasively through the human skull. This was achieved using shear wave transduction to reduce the acoustic impedance mismatch at the interface between the skull and the brain [3]. Although this approach enhanced the degree of transmission across the interface, this did not completely remove interference from reverberations within the skull.

The aim of this paper is to develop the capability for non-invasive, through-steel imaging of dynamic process streams. The methodology entails identifying the signals corresponding to the reverberations in the steel vessel wall and then removing these artefacts from the final image. To increase the practicality of the methodology and reduce industrial costs, the method will not rely on a background measurement of the image scene. Therefore, background subtraction was not a suitable method for identification and removal of the reverberation signals.

The dynamic system that was modelled involved the movement of bubbles rising to the surface of a fluid. A schematic of the ultrasonic hardware coupled to the target application is presented in Figure 1. The aim is to image this system through a 10 mm thick steel wall, which represents a typical pipe wall thickness in an industrial process environment. The array was orientated parallel to the movement of the dynamic reflectors, which moved from the base to the surface of the fluid and the first transmitting element was positioned at the base of the image scene, towards the origin of the y-axis. For clarity in the results presented in this paper, the steel vessel wall was not included in the image scene and the z-axis of the image begins at the steel-fluid interface. To generate an ultrasonic data set of the target image scene, a finite element (FE) model was developed in PZFlex [7] and the images were generated using a GP-GPU on a PC.

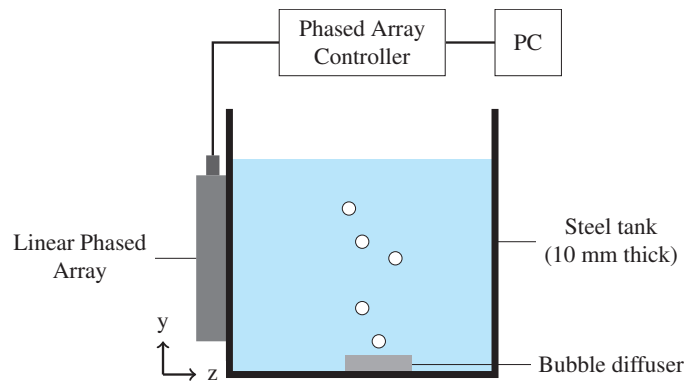


FIGURE 1. Schematic of the ultrasonic hardware coupled to image target.

METHODOLOGY

Data Acquisition and Imaging

To generate high-resolution images of the target scene, the maximum quantity of information about the process must be acquired. To achieve this, Full Matrix Capture (FMC) [8] was chosen as the method of phased array deployment. In FMC each element in the active aperture is sequentially fired and ultrasound reflected from the load medium is received at every element location in the active aperture, therefore maximising the information acquired about the image scene.

The image scene was constructed using the Total Focusing Method (TFM) [8]. The TFM algorithm creates a pixel grid of the image scene and computes the time of flight (TOF) between each transmitting element (T_x), pixel

and receiving element (R_x). Then for each pixel it sums the aperture data from the FMC data set corresponding to each TOF, creating an image that is focussed at every pixel. The TFM algorithm focusses the ultrasonic beam at every pixel in the image by assuming all reflectors are point-like in nature and maps this assumption onto the image pixels. This assumption can lead to pixel aliasing where signals from two different points in space can incorrectly combine, contributing to the value of a pixel where no real reflector exists. In terms of the system described here, this leads to multiples of the vessel-fluid interface interfering with signals within the desired image scene.

Overview of the Simulation Model

A schematic of the FE model is shown in Figure 2, indicating the key design parameters. Note, the image target is stationary as it was not possible to model a dynamic system, however relative to the experimentally measured data acquisition rate (150 FMCs/s), this was a reasonable approximation to an experimental system. The transducer itself was modelled as a pressure loaded array, meaning no transducer effects were modelled and it was assumed the device was perfectly coupled to the outside wall of the steel vessel. This simplified design was used to provide ground truth that any variation between results were purely due to the integrity of the methodology rather than noise from the array design. A two-dimensional model was created because there was symmetry along the yz -plane, provided that the steel vessel was assumed to be infinitely large relative to the array probe.

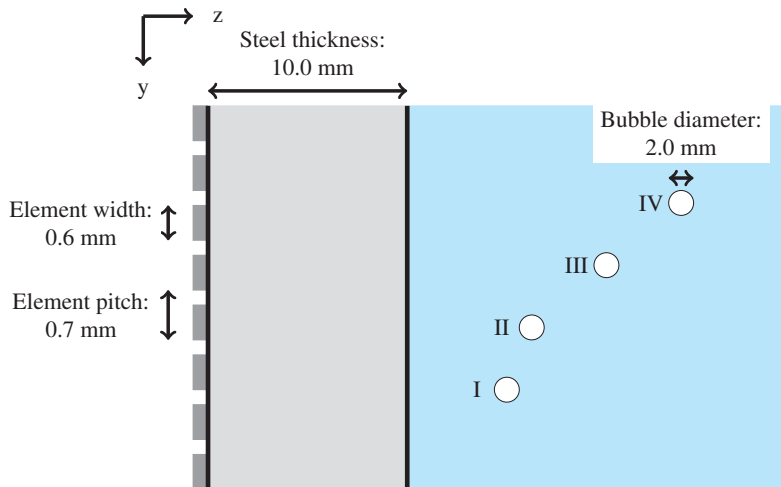


FIGURE 2. Schematic of PZFlex array model used to generate a non-invasive FMC data set.

This model was designed to replicate an experimental apparatus. Given that the image target was dynamic in nature, it was necessary to maximise the FMC acquisition rate with respect to the PAC FIToolbox [9] used for rapid FMC acquisition. However, the FMC acquisition rate was limited by the size of the active aperture. There were 32 channels on the PAC, therefore an active aperture greater than 32 required multiplexing across multiple channels, which led to a reduction in the data acquisition rate. Therefore the FE model was designed as a 32 element array.

The driving conditions of the model were a 5 MHz Blackman-Harris function that was selected to reduce any side-lobe activity. The thickness of the steel vessel wall was set to 10 mm such that it was approximately eight times the ultrasonic wavelength in steel. This meant there was a good separation in time between individual reverberations. The bubble reflectors were modelled as stationary circular voids, such that they reflected 100 % of the ultrasonic energy at their boundaries. The diameter of the bubbles was set to 2 mm, such that they were approximately ten times the ultrasonic wavelength in water, providing strong interaction with the ultrasonic wave. The position of the bubble reflectors was designed so that aliasing would occur with the reverberation signals for reflectors I and III but not reflectors II and IV. The boundary conditions on the model were set to absorbing and the system of interest was placed in water at 25 °C, with the boundaries infinitely extending relative to the temporal range of the ultrasonic reflections. This generated a system with adequate reverberations but without artefacts from the transducer or elsewhere.

Reverberation Pattern Identification

Consider a linear phased array with K elements each positioned precisely the same distance apart, creating a well-defined element pitch, p (mm). This array was coupled directly to the outside of a steel vessel wall, where the array was assumed to be perfectly coupled to the steel and no noise was introduced into the system. The system was simplified further by assuming the steel-fluid interface was parallel to the front face of the array. Therefore, given the vessel wall thickness, z_{steel} (mm), the path length between any two elements and the steel-fluid interface could be determined using Pythagoras' Theorem. If the speed of sound in the steel vessel was assumed to be homogeneous throughout, the TOF for the n^{th} reverberation could be determined from the calculated path length. Given that the reverberating system was geometrically similar, independent of the element that was transmitting, there were only K individual TOF paths to be calculated per n reverberations. Using a known sampling frequency, F_s ($samples/s$), these TOF values were represented in units of samples that were stored in a look-up-table (LUT) of TOF sample values corresponding to the T_x , R_x and the n^{th} reverberation. The number of reverberations to be calculated was determined by the desired image depth into the sample load, where the direct TOF for n reverberations was equal to the TOF to a point in space beyond the steel-fluid interface. A schematic of these parameters is shown in Figure 3 for the first two reverberations.

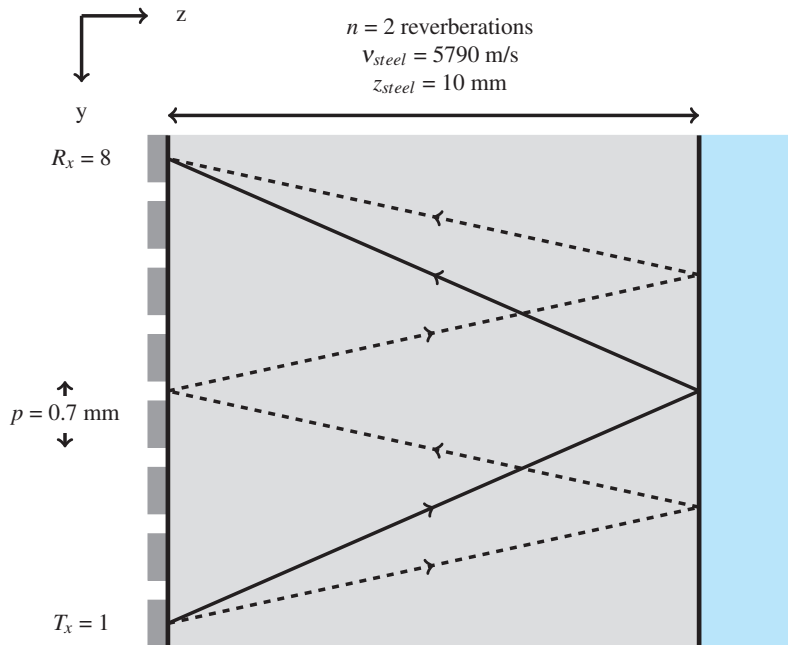


FIGURE 3. Reverberation pattern in steel vessel wall with relevant experimental variables labelled.

Reverberation Gain Correction

Once the LUT has been generated the number of samples corresponding to the pulse length of the transmitted pulse must be determined. The methodology proposed was to compute the Hilbert Transform of the first reverberation and to plot the real component as a function of time. This generated a clear time domain peak of the first reverberation [10], where the pulse length was the time difference (samples) between the first and last samples greater than an arbitrary cut-off value. The cut-off value was selected to be -40 dB because this represents the typical amplitude difference between reverberations and the signals of interest. In addition, it enabled ring-down time to be accounted for in addition to the main reverberation peak.

Next, the FMC data set was passed through a gain filter prior to TFM image construction. For each A-Scan in the FMC data set, the sample corresponding to each reverberation was identified using the LUT and samples following the TOF were windowed before they were reduced in amplitude by an arbitrary value of decibels. The gain reduction process has the impact of reducing signals corresponding to the reverberations but also those signals of interest that

are aliased precisely with these reverberations. Therefore, it was important to manually adjust this parameter with respect to the signal-to-noise ratio required to generate coherent reflectors in the final image. When the reverberation pattern identification was combined with the gain correction filter the method was called the Reverberation Pattern Gain Correction Method (RP-GCM).

To draw quantitative comparisons between the RP-GCM and the regular TFM approach an image window procedure has been developed. The pixels in the image corresponding to the four reflectors were extracted from the full image scene and the coordinates of the pixel with the maximum value in the RP-GCM image were identified. Then the value of this pixel relative to the maximum pixel value in the corresponding full image scene was calculated in units of decibels to demonstrate the relative pixel enhancement.

RESULTS AND DISCUSSION

Determination of Pulse Length

The pulse length was estimated from the first reverberation signal, shown in Figure 4, to be 712 time samples at the -40 dB level. Therefore the first 712 samples after the TOF identified from the LUT were passed through the gain filter.

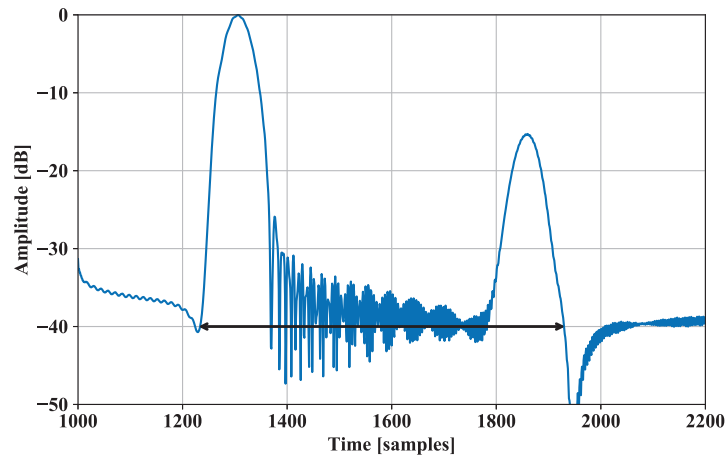


FIGURE 4. Hilbert Transform of the first reverberation, where the double-headed arrow indicates the pulse length used to identify reverberation samples to be passed through the gain filter.

Application of the RP-GCM

The FMC data generated by the FE model were constructed into images of the target region using the TFM. In Figure 5 the TFM image has been constructed without any compensation for the reverberation pattern. At the region corresponding to the steel-fluid interface, the first reverberation was shown as a bright line parallel to the y-axis. This reverberation was the highest amplitude reflection and set the dynamic range of subsequent reverberations in the image as well as the signals of interest. Upon application of the RP-GCM, the amplitude of the reverberations was reduced, however, although the signals from the reverberations were minimised, the pulse length determined previously did not capture the full reflection from the steel-fluid surface. This resulted in some signals corresponding to the second reverberation (the second highest amplitude reverberation) not being passed through the gain filter, offsetting the dynamic range of the final image. If the pulse length was increased further, this would have resulted in signals corresponding to the reflectors of interest also being passed through the gain filter. Therefore a compromise was required to generate adequate images of the process region. Given that the highest amplitude reverberations always occurred in the region closest to the steel-fluid interface, this region (first 2 mm) was declared a dead zone where signals could not be reasonably resolved.

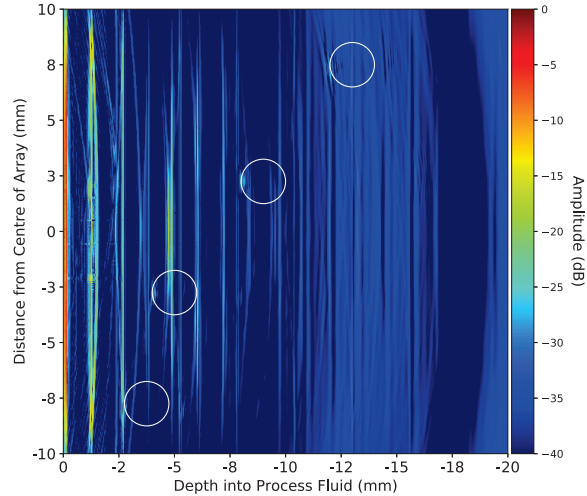


FIGURE 5. TFM image from simulated FMC data without any post-processing prior to image construction. White circles represent the true location of the reflectors.

When the pixels in the dead zone were excluded from the TFM image algorithm, the dynamic range of the region of interest was enhanced. Figure 6(a) shows the TFM image without the application of the RP-GCM and with the dead zone excluded from the image scene. This had the effect of enhancing the amplitude of the subsequent reverberations that in turn off-set the dynamic range of the image relative to the reflectors of interest. However, in Figure 6(b), where the RP-GCM has been applied and the dead zone excluded from the image scene, the reflectors of interest became more visible. The relative improvement between Figures 6(a) and 6(b) for the different reflectors was recorded in Table 1.

TABLE 1. Pixel amplitude enhancement of each of the four reflectors in the FE model.

Reflector	Enhancement (dB)
I	3.86
II	6.26
III	3.67
IV	3.33

Reflectors I and III were less enhanced than II because they were positioned to alias with the TOF of the third and eighth reverberations. Whereas, reflectors II and IV were positioned between the main peaks of the reverberations. The reason reflector IV is less enhanced than reflector II was due to its distance from the reverberating interface. The reverberation signals have already been attenuated by the time they reach this depth into the fluid load, therefore reducing the impact of the RP-GCM. In all cases, the amplitude of the reflectors has been enhanced by the RP-GCM and this shows that the RP-GCM can adequately remove interference corresponding to a reverberation pattern while maintaining the signals corresponding to reflectors of interest. However, one reverberation at 12 mm in Figure 6(b) could still be seen. The gain-reduced amplitude of this reverberation was on the same level as the reflectors of interest. Therefore, the dynamic range of the image could not be adjusted to compensate for this without the loss of reflector I closest to the steel-fluid interface.

CONCLUSIONS AND FUTURE WORK

A methodology has been proposed to identify and minimise signals corresponding to the reverberation pattern in a steel vessel wall. The findings were verified using a simulated FMC data set, where results indicated a minimum 3 dB

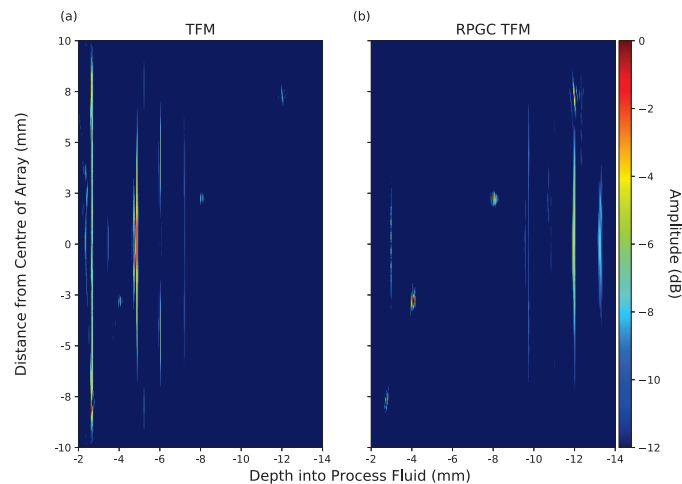


FIGURE 6. TFM images of the process region generated from simulated FMC data with the dead zone excluded from the image scene: (a) TFM image without post-processing of the FMC data and (b) TFM with the RP-GCM applied.

enhancement in pixel amplitude of the reflectors of interest. These findings will provide the opportunity to develop non-invasive through-steel imaging of dynamic process streams using ultrasonic phased arrays. The next stage of the research is to investigate the impact of varying vessel wall thickness and to deploy the methodology using an experimental apparatus.

ACKNOWLEDGMENTS

The authors would like to thank the Engineering and Physical Sciences Research Council (grant number EPM5076471) and BP Chemicals Limited for their support and industrial direction.

REFERENCES

- [1] B. Drinkwater and P. Wilcox, *NDT & E International* **39**, 525 – 541 (2006).
- [2] T. Lardner, M. Li, R. Gongzhang, and A. Gachagan, “A new speckle noise suppression technique using cross-correlation of array sub-apertures in ultrasonic nde of coarse grain materials,” in *Review of Progress in Quantitative Non-destructive Evaluation*, Vol. 32 (AIP Publishing, 2013), pp. 865 – 871.
- [3] G. Clement, P. White, and K. Hynynen, *The Journal of the Acoustical Society of America* **115**, 1356–1364 (2004).
- [4] J. Bamberger and M. Greenwood, *Food Research International* **37**, 621 – 625 (2004).
- [5] R. Carvalho, O. Venturini, E. Tanahashi, F. Neves, and F. Frana, *Experimental Thermal and Fluid Science* **33**, 1065 – 1086 (2009).
- [6] S. Cunha, F. Jurandyr, M. Farias, J. Faccini, C. Lamy, and J. Su, “High speed ultrasonic system to measure bubbles velocities in a horizontal two-phase flow,” in *International Nuclear Atlantic Conference-INAC*, Vol. 2009 (2009).
- [7] PZFlex, OnScale, USA. 2018.
- [8] C. Holmes, B. Drinkwater, and P. Wilcox, *NDT & E International* **38**, 701 – 711 (2005).
- [9] FIToolbox, Diagnostic Sonar Limited, Livingston, UK. 2018.
- [10] T. Namas and M. Dogruel, “A feasible and accurate technique for determining the time-of-flight in ultrasonic distance measurements,” in *ELMAR, 2008. 50th International Symposium*, Vol. 1 (IEEE, 2008), pp. 337–340.